Nonenzymatic Reduction of Hydrogen Peroxide Produced during the Bioelectrocatalysis of Glucose Oxidase on Urchin-like Nanofibrillar Structures of Cu on Au Substrates

A. Vijayalakshmi, R. Karthikeyan, and Sheela Berchmans*

Central Electrochemical Research Institute (CECRI-CSIR), Karaikudi-630006, Tamilnadu, India

Received: May 4, 2010; Revised Manuscript Received: October 25, 2010

This work describes the nonenzymatic reduction of hydrogen peroxide on urchin-like nanofibrillar structures of Cu formed on gold substrates modified by a self-assembled monolayer (SAM) of *p*-mercaptobenzoic acid. Because the detection is based on the electrochemical reduction, the method is less prone to interference from easily oxidizable biologically important compounds such as dopamine, uric acid, and ascorbic acid. This method is extended to the detection of glucose by immobilizing glucose oxidase on the nanocomposite electrode with the help of chitosan. The linear detection range for glucose is 100 nM to 1800 nM. Sensitivity of detection is 1.99 nA/nM. The Michaelis−Menten constant is very low (125 nM), indicating high binding affinity of the enzyme to the substrate.

1. Introduction

Development of electrochemical biosensors is very important because of the advantages offered by the specificity of biochemical recognition and by the convenience of electrochemical signal transduction. Oxidoreductase enzymes such as glucose oxidase, lactate oxidase, and choline oxidase catalyze the oxidation of their specific substrates by molecular oxygen with concomitant generation of H_2O_2. This has led to the development of optical,[1−3] chemiluminescent,[4,5] and electrochemical[6] biosensors for different oxidoreductase-dependent substrates based on H_2O_2 transduction. Electrochemistry has been proved to be an inexpensive and effective way to examine reactions of many analytes. H_2O_2 transductions can be carried out either through electrochemical oxidation or through electrochemical reduction. The electrochemical oxidation of hydrogen peroxide is, however, made difficult by slow electrode kinetics on many electrode materials. As a result, high overpotentials are required which makes the detection prone to interference from substrates such as dopamine, paracetamol, ascorbate, and urate.[7] To overcome these problems, two main approaches have been explored. One promising method, to suppress the interference and to improve the sensitivity of the sensors, involves the use of the bienzymes oxidase and peroxidase.[8] Second, the integration of organic and inorganic materials on nanoscale is a promising method for obtaining unusual functional materials. Artificial combinations of the solid-state properties of inorganic materials and the chemical or biofunctional properties of the organic part may produce a unique function. In essence, inorganic materials with superior selective catalytic properties toward the electrochemical reduction of hydrogen peroxide can be incorporated along with an organic hybrid containing glucose oxidase.[9−11] Bioelectrocatalytic reduction of H_2O_2 by horseradish peroxidase[12−14] and heme protein[15] functionalized electrodes are normally used for developing biosensors for analytes dependent on oxidoreductases. With the advent of nanotechnology and hybrid materials, nanostructured inorganic hybrid materials have become the substitutes for peroxidases. The presence of nanoparticles in electrochemical sensors can decrease the overpotentials of many analytes at common unmodified electrodes.[16] In the past decade, several electrochemical biosensors, which were modified with metal nanomaterials, have been studied and analyzed for their response to hydrogen peroxide and these nanomaterials amplified the signal for the transduction of H_2O_2 by enzymatic methods. These include gold,[17] silver,[18−20] platinum,[21] and metallic oxides such as MnO_2.[22] On the contrary, only a few examples of chemically modified electrodes based on metal nanoparticles have been reported for the direct analytical determination of hydrogen peroxide. Platinum,[23,24] copper oxide,[25] and silver[7] nanoparticles have been reported for the direct determination of hydrogen peroxide. Inorganic nanostructured Prussian blue has also been used for the direct analytical determination of H_2O_2 based on electrochemical reduction.[9,10] Further, in recent years, organic hybrid materials such as silica and chitosan gain interest as matrixes for enzyme immobilization owing to the synergy resulting from the combination of the intrinsic properties of the two components.[26,27] In this work we have developed an integrated chemical system consisting of heterogeneous multiphase systems for the immobilization of glucose oxidase and for the transduction of hydrogen peroxide. We describe an analytical protocol for sensing hydrogen peroxide based on its electrochemical reduction on a Cu−SAM nanocomposite electrode. Urchin-like Cu nanofibrillar structures are formed by electrochemical deposition on a gold electrode modified by a self-assembled monolayer of *p*-mercaptobenzoic acid, and they are found to be an effective catalyst for the electrochemical reduction of hydrogen peroxide. The enzyme immobilization was carried out using the biopolymer film chitosan, a unique organic hybrid material which, due to its various glucose amine groups, can effectively trap anionically charged glucose oxidase molecules. The present approach for the detection of glucose helps to alleviate the following difficulties normally encountered in the enzymatic analysis of glucose.

1. The hydrogen peroxide liberated in the enzymatic release is conventionally estimated by following the electrochemical oxidation of H_2O_2 which occurs at high overpotentials, and therefore glucose estimation is prone to interference from other oxidizable compounds. This problem is completely overcome

* Corresponding author. Tel: +91 4565 227550; fax: +91 4565 227779; e-mail: sheelaberchmans@yahoo.com.

10.1021/jp109126q
Published on Web 12/01/2010

in the present analysis by following the electrochemical reduction of hydrogen peroxide.

$$\text{glucose} + O_2 \xrightarrow{\text{glucose oxidase}} \text{gluconic acid} + H_2O_2$$

2. Glucose detection using the bienzymatic approach (glucose oxidase + peroxidase) also involves transduction of hydrogen peroxide reduction. Normally, stability problems are faced with enzymatic detection when repeated trials are carried out. Instead of addressing the stabilities of two enzymes, we can have one enzymatic reaction and one electrocatalytic reaction for carrying out the whole process of sensing, which will bring out the synergistic effect of the hybrid materials. Further, immobilization of two enzymes in two spatially separated planes is quite challenging.

$$\text{glucose} + O_2 \xrightarrow{\text{glucose oxidase}} \text{gluconic acid} + H_2O_2$$

$$2H_2O_2 \xrightarrow{\text{peroxidase}} 2H_2O + O_2$$

3. Our method of preparation has resulted in interesting urchin-shaped nanofibrillar Cu structures which exhibit very good electrocatalytic properties toward hydrogen peroxide reduction. Hence, glucose detection can be carried out at low overpotentials with no possibility of interference. Further, the structure-directing effect of the mercaptobenzoic acid SAM layer to form the nanofibrillar structures is an interesting aspect of this work.

2. Experimental Section

2.1. Preparation of Cu Nanostructures on SAM-Modified Electrodes. The preparation of the metal−SAM nanocomposite layer has already been reported by us.[28,29] Briefly, a gold slide (Au 111) electrode (1000 Å Au coating on Si wafers with an intermediate adhesion layer of 100 Å thick Ti, procured from Lance Goddard Associates, Foster City, CA) of area 12 mm^2 was used for all the experiments. After thorough cleaning, the gold plates are immersed in 1 mM *p*-mercaptobenzoic acid overnight for SAM formation. The SAM-modified electrode is immersed in 1 mM $CuSO_4$ for 15 min during which Cu^{2+} ions are chemically preconcentrated on the Au−SAM electrode. The preconcentrated Cu^{2+} ions are electrochemically reduced by applying a potential of −0.6 V Vs Hg/Hg_2SO_4 for 15 min in 0.5 M sulfuric acid. This procedure results in the formation of the Cu−SAM nanocomposite electrode. The effect of variation of preconcentration time and concentration of $CuSO_4$ used for preconcentration are also investigated.

2.2. Immobilization of Glucose Oxidase on the Cu−SAM Nanocomposite Electrode. A 0.5% solution of chitosan (gift sample from Everest Biotech) in concentrated HCl solution is neutralized by adding NaOH to a final pH of 6.5−7.0. The Cu−SAM nanocomposite is immersed in the chitosan solution for 3 h. Glucose oxidase (4 mg/mL) solution is prepared in phosphate buffer (pH 7.0). The Cu−SAM nanocomposite electrode modified by chitosan is immersed in the enzyme solution overnight for enzyme immobilization.

2.3. SEM Characterization. SEM measurements are made using a Hitachi model S3000-H.

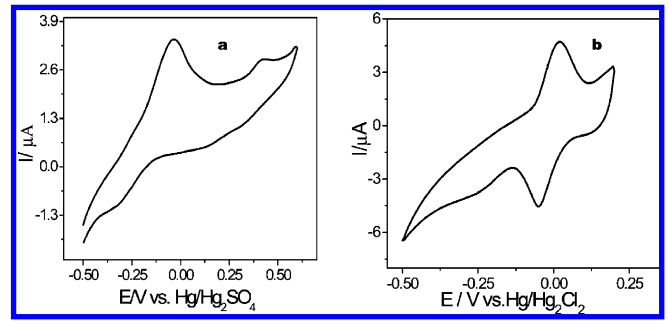

Figure 1. Cyclic voltammogram for Cu−SAM nanocomposite electrode in (a) 0.5 M sulfuric acid, (b) phosphate buffer pH = 7.0; scan rate = 50 mV/s.

2.4. XPS Characterization. X-ray photoelectron spectroscopic studies were carried out using a Multilab 2000 model, Thermo Scientific, UK. A source of Al Kα having a binding energy of 1486.4 eV was used for the study. Initially a full scan from −10 to 1100 eV was performed and later on individual scans of 50−100 eV having a step energy of 0.5 eV were carried out in order to analyze the presence of specific elements.

2.5. Electrochemical Measurements. PGSTAT 302N (Autolab) was used for the electrochemical measurements. The electrochemical characterization of the Cu-nanocomposite electrode was performed in 0.5 M sulfuric acid with Hg/Hg_2SO_4 as the reference electrode and Pt counter electrode. The electrochemical detection of hydrogen peroxide and the enzymatic detection of glucose were performed in phosphate buffer (pH = 7.0) with Hg/Hg_2Cl_2 as the reference electrode and Pt counter electrode.

3. Results and Discussion

3.1. Characterization of the Cu−SAM Nanocomposite Electrode. Figure 1 shows the response for the Cu−SAM nanocomposite electrode (based on the protocol described in the Experimental Section) formed on the gold substrate modified with a self-assembled monolayer of *p*-mercaptobenzoic acid on the gold electrode. The formation of Cu deposits can be seen by characteristic peaks appearing at 0.429 V (anodic) and −0.034 V (anodic) and −0.332 V (cathodic) vs Hg/Hg_2SO_4. The anodic peak appearing at 0.429 V corresponds to underpotentially deposited Cu (upd), and the peak appearing at −0.034 V corresponds to bulk Cu. The peak separation for bulk Cu is greater than 200 mV, and hence the electron transfer is irreversible. Similar behavior has been observed by us[28] when such Cu films were prepared for the galvanic replacement of noble metals. The upd Cu is stabilized in the presence of SAM layers formed on Au (111) substrates, and we have shown earlier that the subsequent derivatization of the films by Pt has led to the preparation of films with superior catalytic properties. In the present work, the Cu nanofibrillar deposit formed on SAM is used for the detection of H_2O_2. It is demonstrated that the electrocatalysis of H_2O_2 occurs at lower overpotentials compared to silver nanostructures formed by a similar method (see Supporting Information). The organic monolayer of *p*-mercaptobenzoic acid self-assembled on Au (111) has some structure-directing and stabilizing effect on the Cu deposits, and hence interesting shapes are obtained. Figure 1b corresponds to the voltammetric response of the Cu−SAM nanocomposite in phosphate buffer (pH = 7.0). The Cu redox peak appears more reversible compared to acidic pH and occurs at 0.098 V (anodic) and 0.054 V (cathodic) at a scan rate of 50 mV/s.

Figure 2 shows SEM images of the Cu−SAM nanocomposite electrode under different conditions of chemical preconcentration

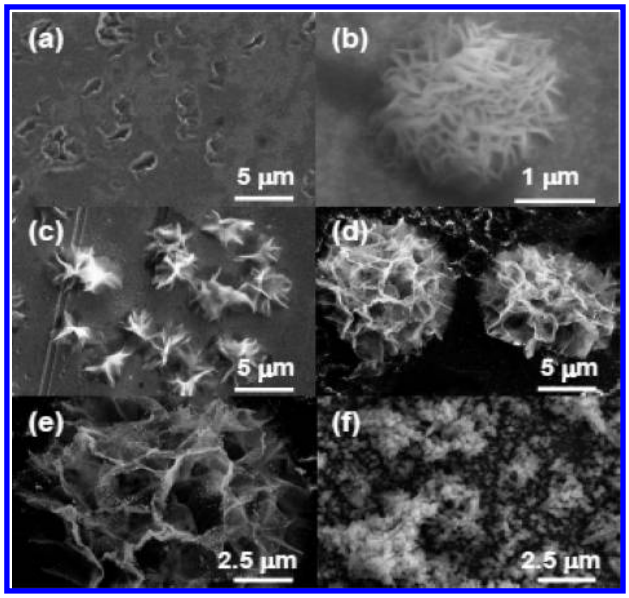

Figure 2. (a−e) SEM images of the Cu nanocomposite electrode. (a) Preconcentration time = 5 min; [$CuSO_4$] = 1 mM. (b) Preconcentration time = 15 min; [$CuSO_4$] = 1 mM. (c) Preconcentration time = 30 min; [$CuSO_4$] = 1 mM. (d) Preconcentration time = 2 h; [$CuSO_4$] = 5 mM. (e) Prepared under the conditions given in d and then treated with phosphate buffer. In all the cases, electrochemical deposition was carried out at −0.6 V for 15 min. (f) 1 mM Cu^{2+} ions deposited under a constant current density of 10 $\mu A/cm^2$ on a Au−SAM electrode.

of copper ions. Figure 2a corresponds to the copper deposit formed when Cu^{2+} ions are chemically preconcentrated on the Au−SAM film using 1 mM Cu SO_4 solution for 5 min followed by electrochemical deposition for 15 min. Figure 2b corresponds to the copper deposit formed when Cu^{2+} ions (1 mM $CuSO_4$) are chemically preconcentrated for a duration of 15 min followed by electrochemical deposition for 15 min. Figure 2c corresponds to the copper deposit when Cu^{2+} ions (1 mM $CuSO_4$) are chemically preconcentrated for a duration of 30 min followed by electrochemical deposition for 15 min. Figure 2d corresponds to a preconcentration time of 2 h ($CuSO_4$, 5 mM) followed by electrochemical deposition for 15 min. Figure 2e corresponds to the morphology of the Cu−SAM composite after treating with phosphate buffer. The mechanism of formation of the Cu deposit has been already discussed in our earlier paper.[29] The carboxylate groups complex the Cu^{2+} cations, and they become preconcentrated on the SAM structure. The electrochemical deposition at −0.6 V deposits Cu atoms on the surface of the Au−SAM substrates. Initially, Cu atoms nucleate on the surface. The structure-directing effect of the underlying organized SAM dictates the growth of the Cu deposits in the form of urchins (see Scheme 1). Depending on the preconcentration time, the concentration of $CuSO_4$ solution used for preconcentration, and deposition time, interesting morphologies are obtained. When a concentration of 1 mM $CuSO_4$ was used for preconcentration for a period of 5 min, fibrillar structures start to appear, as seen by the "frog leg"-like structures in Figure 2a. When the preconcentration time increases to 15 min, fully grown urchin-like structures are clearly seen (Figure 2b). The urchin is made of nanofibrillar structures where the diameter of each nanofiber is ∼50 nm and the length is ∼0.75−1 μm. A fully grown urchin has a diameter of 2.5 μm. A further increase in the preconcentration time (30 min) also reveals urchin-like structures (Figure 2c). When a high concentration of $CuSO_4$ (5 mM) solution is used for preconcentration for a period of 2 h, we see the urchins grow further in size (7 μm). Similar structure is seen after exposing the substrate to phosphate buffer (Figure 2e). Uniform growth of urchin-like structures of ZnO has been reported recently on ITO substrates where PSS spheres are used as templates for the formation of urchins, and the deposition of ZnO has been carried out under constant current density.[30] The PSS templates direct the growth of urchins. A similar phenomenon is observed here under constant reduction potential. We also carried out deposition of Cu in the presence of SAM using constant current density, and we observed uniform deposition of Cu and that the size of the structures vary between 100−125 nm (Figure 2f). Urchin-like structures are not observed during galvanostatic deposition. Preconcentration of Cu^{2+} ions on the SAM layer followed by electrochemical deposition at constant potential leads to urchin-like structures. However, the organization of urchins directed by SAM is poor compared to PSS templates in the case of ZnO.[30] Further, the main emphasis in the present work is to explore use of Cu structures for their sensing capabilities.

The formation of the Cu deposit is also confirmed by XPS measurements of the characteristic Cu peaks. The presence of the copper on the surface of the gold plate electrode was confirmed by XPS which shows two peaks at 933 eV and 952 eV corresponding to the presence of Cu^0 on the surface of the electrode (Figure 3).

3.2. Detection of Hydrogen Peroxide. Figure 4 shows the response of Cu−SAM nanocomposite electrode for stepwise additions of different concentrations of hydrogen peroxide in phosphate buffer (pH = 7). The cyclic voltammogram corre-

SCHEME 1: (A) Chemical Preconcentration of Cu^{2+} Ions on Au Substrate Modified by a Self-Assembled Monolayer (SAM) of *p*-Mercaptobenzoic Acid. (B) Electrochemical Reduction of Cu^{2+} Ions (preconcentration time = 5 min; [Cu^{2+}] = 1 mM). (C) Urchin-like Cu nanofibrillar structure (preconcentration time = 15−30 min; [Cu^{2+}] = 1 mM)

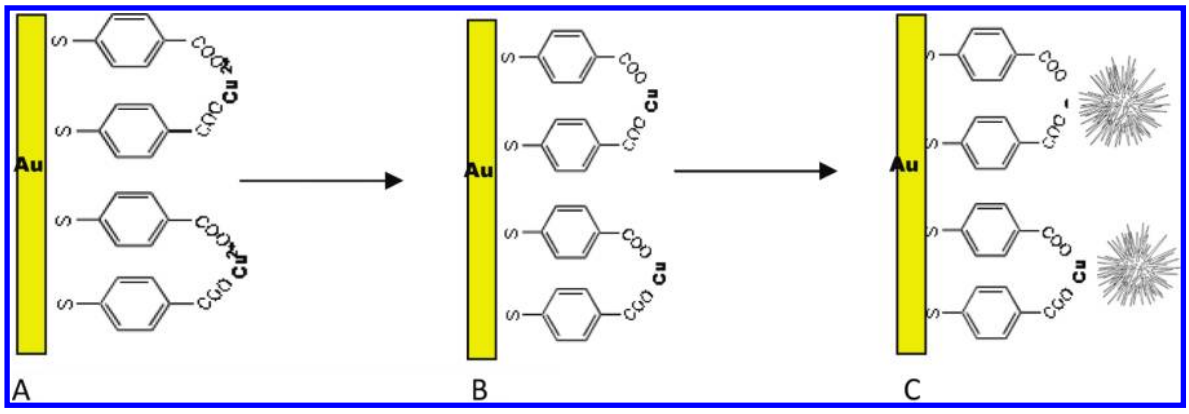

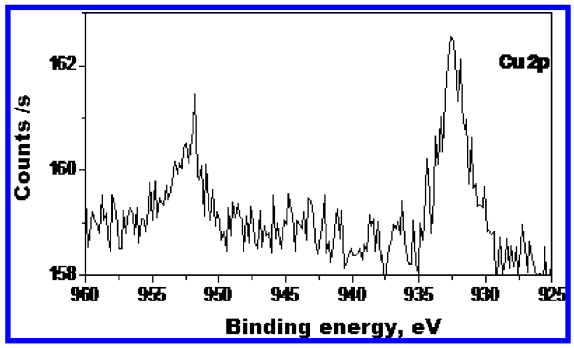

Figure 3. XPS of Cu 2p response for the Cu−SAM nanocomposite.

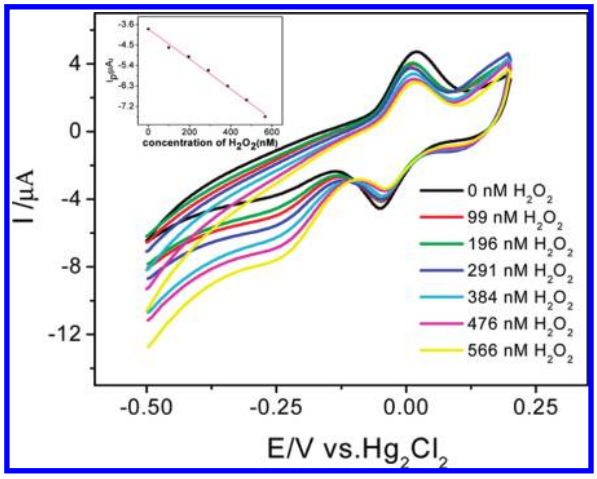

Figure 4. Cyclic voltammograms of the Cu nanocomposite electrode for different concentrations of hydrogen peroxide in phosphate buffer pH = 7.0. Scan rate 50 mV/s.

sponding to zero addition of H_2O_2 is the innermost curve. This voltammogram exhibits the cathodic peak corresponding to Cu at −0.052 V vs Hg/Hg_2Cl_2. For each addition of hydrogen peroxide, the current shows a corresponding increase in the voltammogram, indicating the catalytic reduction of hydrogen peroxide. The electrochemical reduction of hydrogen peroxide occurs at −0.250 V. The peak potential for reduction shifts slightly to positive values for further additions. Compared to the electrochemical reduction potential of hydrogen peroxide on Ag and Au nanoparticle-modified electrodes,[7,31−33] the overpotential for reduction is lower in the case of the Cu−SAM nanocomposite electrode. This shows that the electrochemical reduction of H_2O_2 in phosphate buffer is facile at neutral pH on the Cu−SAM nanocomposite electrode. Similar experiments with the Ag−SAM nanocomposite electrode carried out by us revealed the requirement of higher overpotentials for reduction (see Supporting Information). Hence, our modification of Au substrate with Cu nanofibrillar structure is a good analytical platform for the detection of H_2O_2. The linear range of detection shown in Figure 4 is 90 nM to 500 nM. The correlation coefficient is 0.99, and the sensitivity of detection is 6.6 nA/nM. The detection can be, however, carried out over a broad range of concentrations from 90 nM to 2500 nM. The voltammagrams showing the detection of H_2O_2 over different concentration ranges are presented in Figure 5. The onset of reduction starts at the reduction potential of Cu. This is revealed in the voltammograms presented in Figure 5a−d. For three concentration ranges (a−c), the reduction occurs at a lower potential of −0.166 V. The sensitivities of detection corresponding to Figure 5a−c are 5.71 nA/nM, 21.71 nA/nM, and 30.5 nA/nM, respectively. The correlation coefficient for the linear range is 0.98 ± 0.07. The reduction potential shifts to −0.269 V (Figure 5d) in the concentration range 2537−2754 nM. Saturation is observed around 2600 nM. As discussed in Introduction, the detection of hydrogen peroxide based on electrochemical reduction removes the possibility of interference from biologically important analytes such as dopamine, ascorbic acid, uric acid, etc. There is no possibility of interference from species that are reduced at the modified electrode, as the hydrogen peroxide reduction occurs at low overpotentials. Some of the possible interferents are oxygen, nitrate, nitrite, ammonia, hydroxylamine, etc. The electrochemical reduction kinetics of these interferents at neutral pH is very sluggish and is favorable only under acidic conditions especially for nitrate, nitrite, hydroxylamine, and oxygen. Our control experiments with respect to these interferents show complete absence of interference from these species. Hydroxylamine and ammonia exhibit a current increase in the anodic direction quite positive to our detection potentials (see Supporting Information). Further nonenzymatic oxidation of carbohydrates, especially glucose, has been carried out by other researchers using Cu particles embedded on polymeric supports, and in all the cases the detection has been carried out under alkaline conditions at high overpotentials where the interference will be maximum.[34−37] Further, the pH used is always alkaline. However, the Cu−SAM nanocomposite electrode prepared by us is used in the reduction of hydrogen peroxide at neutral pH, and hence sugars such as glucose and fructose have no possibility of getting oxidized at the Cu−SAM nanocomposite electrode. Our experimental results also support the same conclusion (see Supporting Information).

The amperometric detection of hydrogen peroxide was carried out at −0.250 V vs Hg/Hg_2Cl_2. The linear range of detection is 90 nM to 1000 nM. Each step in the amperometric curve corresponds to the addition of 90 nM. The linear graph between current vs concentration is presented in the inset. The sensitivity of detection is 2.7 nA/nM, and the correlation coefficient is 0.98 (Figure 6).

3.3. Detection of Glucose. The voltammogram corresponding to the response of the Cu−SAM nanocomposite-modified electrode further functionalized with a layer of chitosan-containing immobilized glucose oxidase is shown in Figure 7. The peaks corresponding to the direct electron transfer of the FAD groups of the enzyme can be seen as a very broad peak with two overlapping peaks occurring at 0.198 V and at 0.39 V at 5 mV/s in the anodic direction. As the scan rate is increased to 25 mV/s, the two peaks overlap and appear as a broad single peak. With the help of the chitosan matrix, the glucose oxidase molecules are effectively immobilized in a favorable orientation so that the electroactivity of the FAD groups can be recorded. However, the enzyme molecules could not turnover glucose under anaerobic conditions. Hence, direct bioelectrocatalysis of glucose could not be carried out using this electrode. However, in the presence of electron acceptors such as oxygen, glucose can be bioelectrocatalytically oxidized to yield gluconic acid and hydrogen peroxide, and the latter could undergo kinetically facile electrochemical reduction at the underneath Cu−SAM nanocomposite electrode. This approach is free from interference effect as mentioned earlier in section 3.2. Hence, we have resorted to the transduction of hydrogen peroxide in the cathodic direction for the sensing of glucose (see Figure S4 in Supporting Information).

Figure 8 corresponds to the amperometric response for the Cu−SAM nanocomposite electrode modified by a glucose oxidase layer immobilized using chitosan. Each step in the

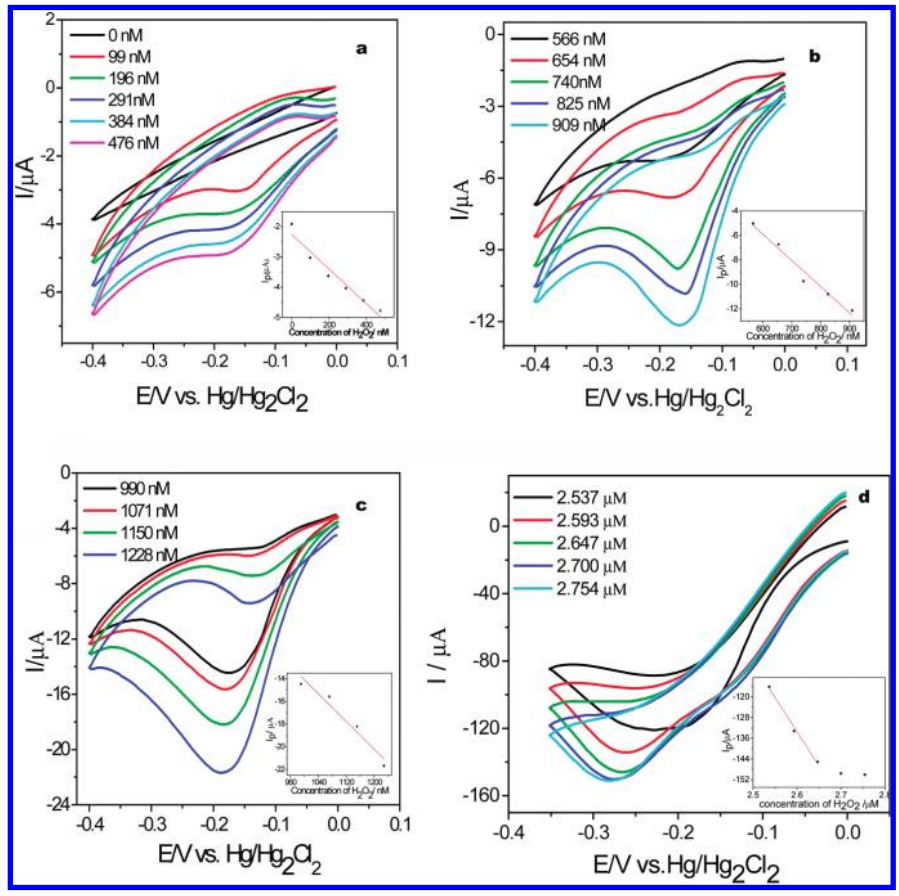

Figure 5. Cyclic voltammograms for the catalytic reduction of H_2O_2 over different concentration ranges in phosphate buffer pH = 7.0. (a) 90 nM to 476 nM. (b) 566−909 nM. (c) 990 to 1228 nM. (d) 2537 to 2750 nM at 50 mV. Scan rate = 50 mV/s.

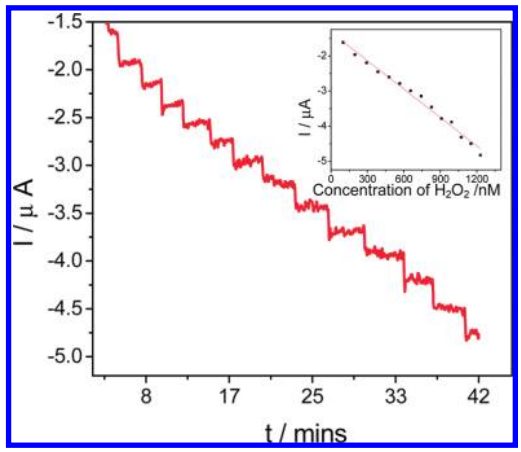

Figure 6. Amperometric curve for standard additions of hydrogen peroxide on the Cu nanocomposite electrode in phosphate buffer pH = 7.0. Applied potential = −0.25 V. Each step corresponds to the addition of 99 nM hydrogen peroxide.

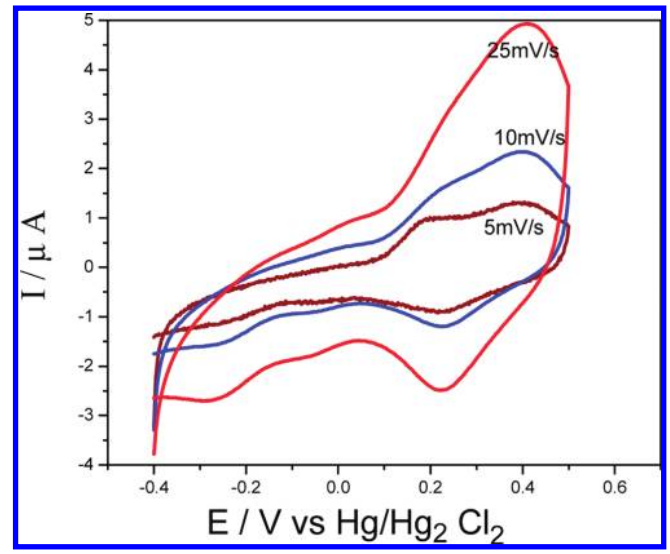

Figure 7. Cyclic voltammetric response for the Cu−SAM nanocomposite electrode further functionalized with glucose oxidase using chitosan at different scan rates, exhibiting the electroactivity of the FAD groups of the enzyme.

amperometric curve corresponds to the addition of 190 nM glucose in phosphate buffer (pH = 7.0). The corresponding linear graph between current vs concentration is shown in the inset. The current approaches saturation nearing a concentration of 1000 nM. The Michaelis−Menten constant was calculated to be around 125 nM. This suggests very high affinity of the enzyme toward substrate. The sensitivity of detection is 1.9 nA/nM. The linear detection range is from 100 nM to 1800 nM.The interference was found to be practically negligible under the potentials used.

4. Conclusion

This paper describes a new analytical strategy for the detection of hydrogen peroxide based on the electrochemical reduction on a Cu−SAM nanocomposite electrode which is free from interference arising from easily oxidizable biologically important analytes such as ascorbic acid, dopamine, and uric acid. The urchin-like Cu nanostructures consisting of nanofibrillar Cu are useful to detect hydrogen peroxide at a lower

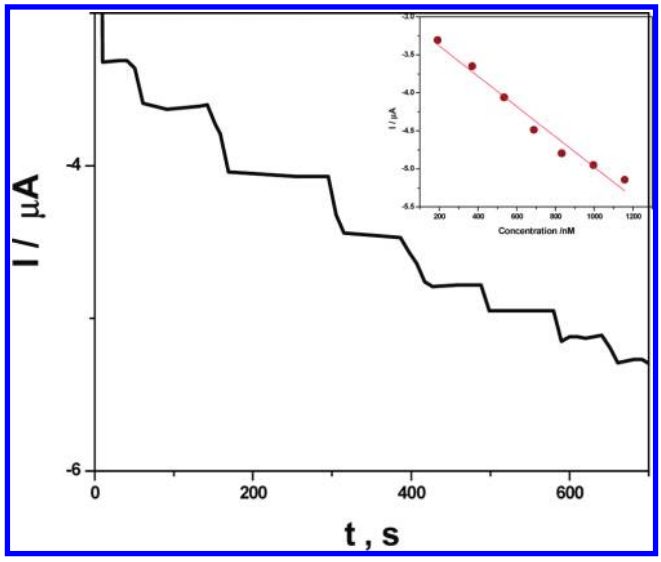

Figure 8. Amperometric curve for different additions of glucose on the Cu−SAM nanocomposite electrode further functionalized with glucose oxidase using chitosan in phosphate buffer pH = 7. $E_{applied}$ = −0.25 V. Each step corresponds to the addition of 190 nM glucose.

overpotential of −0.250 V. The overpotential observed for the electrochemical reduction of hydrogen peroxide is lower compared to the electrodes modified using Ag and Au nanostructures. The transduction of H_2O_2 using the Cu−SAM nanocomposite platform can be extended to the enzymatic sensing of glucose by further modifying the Cu−SAM nanocomposite electrode by immobilizing glucose oxidase using chitosan. The electrode further modified by a layer of glucose oxidase immobilized in chitosan is demonstrated to be a very good platform for sensing glucose.

Acknowledgment. The authors acknowledge Department of Biotechnology, New Delhi, India, for funding this work.

Supporting Information Available: Characterization of Ag−SAM nanocomposite-modified Au substrate by cyclic voltammetry, catalytic reduction of H_2O_2 on Ag nanocomposite-modified Au substrate characterized by cyclic voltammetry and amperometry, effect of addition of glucose to the Au−SAM−Cu−(chitosan + glucose oxidase electrode), and the effect of interference. This information is available free of charge via the Internet at http://pubs.acs.org.

References and Notes

(1) Wu, M.; Lin, Z.; Schaeferling, M.; Duerkop, A.; Wolfbeis, O. S. *Anal. Biochem.* **2005**, *340*, 66.
(2) Wolfbeis, O. S.; Schaeferling, M.; Duerkop, A. *Microchim. Acta* **2003**, *143*, 221.
(3) Gill, R.; Bahshi, L.; Freeman, R.; Willner, I. *Angew. Chem., Int. Ed.* **2003**, *47*, 1676.
(4) Shi, C. G.; Xu, J. J.; Chen, H. Y. *J. Electroanal. Chem.* **2007**, *610*, 186.
(5) Wang, J. *Chem. Rev.* **2008**, *108*, 814.
(6) Zhou, G. J.; Wang, G.; Xu, J. J.; Chen, H. Y. *Sens. Actuators, B* **2002**, *81*, 334.
(7) Welch, C. M.; Banks, C. E.; Simon, A. O.; Compton, R. G. *Anal. Bioanal. Chem.* **2005**, *382*, 12.
(8) Manesh, K. M.; Santhosh, P.; Uthayakumar, S.; Gopalan, A. I.; Lee, K. P. *Biosens. Bioelectron.* **2010**, *25*, 1579.
(9) Kusakari, A.; Izumi, M.; Ohnuki, H. *Colloids Surf., A* **2008**, *321*, 47.
(10) Gonçales, V. R.; Salvador, R. P.; Alcântara, M. R.; Córdoba de Torres, S. I. *J. Electrochem. Soc.* **2008**, *155*, K140.
(11) Ohnuki, H.; Saiki, T.; Kusakari, A.; Endo, H.; Ichihara, M.; Izumi, M. *Langmuir* **2007**, *23*, 4675.
(12) Ohara, T. J.; Vreeke, M. S.; Battaglini, F.; Heller, A. *Electroanalysis* **1993**, *5*, 825.
(13) Su, X.; O'Shea, S. J. *Anal. Biochem.* **2001**, *299*, 241.
(14) Asberg, P.; Inganas, O. *Biosens. Bioelectron.* **2003**, *19*, 9.
(15) Narvaez, A.; Dominguez, E.; Katakis, I.; Katz, E.; Ranjit, K. T.; Ben-Dov, I.; Willner, I. *J. Electroanal. Chem.* **1997**, *430*, 227.
(16) Ordeig, O.; Banks, C. E.; J.del Campo, F.; Munoz, F. X.; Davis, J.; Compton, R. G. *Electroanalysis* **2006**, *18*, 1672.
(17) Shiyi, X.; Bo, P.; Xiaozu, H. *Biosens. Bioelectron.* **2007**, *22*, 1807.
(18) Liu, Y.; Hu, L. M.; Yang, S. Q. *Microchim. Acta* **2008**, *160*, 357.
(19) Wang, F.; Yuan, R.; Chai, Y.; Tang, D. *Anal. Bioanal. Chem.* **2007b**, *387*, 709.
(20) Wu, S.; Zhao, H.; Ju, H.; Shi, C.; Zhao, J. *Electrochem. Commun.* **2006**, *8*, 1197.
(21) Wang, A.; Ye, X.; He, P.; Fang, Y. *Electroanalysis* **2007a**, *19*, 1603.
(22) Bai, Y.; Du, Y.; Xu, J.; Chen, H. *Electrochem. Commun.* **2007**, *9*, 2611.
(23) You, T. Y.; Niwa, O.; Tomita, M.; Hirono, S. *Anal. Chem.* **2003**, *75*, 2080.
(24) Han, J. H.; Boo, H.; Park, S.; Chumg, T. D. *Electrochim. Acta* **2006**, *52*, 1788.
(25) Miao, X.; Yuan, R.; Chai, Y.; Shi, Y.; Yuan, Y. *J. Electroanal. Chem.* **2008**, *612*, 157.
(26) Xinhao, Y.; Hua, L.; Gong, H.; Tan, S. N. *Anal. Chim. Acta* **2003**, *478*, 67.
(27) Ji, X.; Ren, J.; Ni, R.; Liu, X. *Analyst* **2010**, *135*, 2092.
(28) Berchmans, S.; Arunkumar, P.; Lalitha, S.; Yegnaraman, V.; Bera, S. *Appl. Catal., B* **2009**, *88*, 557.
(29) Arunkumar, P.; Berchmans, S.; Yegnaraman, V. *J. Phys. Chem. C* **2009**, *113*, 8378.
(30) Elias, J.; Lévy-Clément, C.; Bechelany, M.; Michler, J.; Wang, G.; Wang, Z.; Philippe, L. *Adv. Mater.* **2010**, *22*, 1.
(31) Zhao, B.; Liu, Z.; Liu, Z.; Liu, G.; Li, Z.; Wang, J.; Dong, X. *Electrochem. Commun.* **2009**, *11*, 1707.
(32) Guas ito, M. R.; Flippo, E.; Malitesta, C.; Manno, D.; Serra, A.; Turco, A. *Biosens. Bioelectron.* **2008**, *24*, 1057.
(33) Hamer, M.; Carballo, R. R.; Rezzano, I. N. *Electroanalysis* **2009**, *21*, 2133.
(34) Casella, I. G.; Gatta, M.; Guascito, M. R.; Cataldi, T. R. I. *Anal. Chim. Acta* **1997**, *357*, 63.
(35) Mastsubara, H.; Ondo, T. K.; Kanno, W.; Hodouchi, K.; Yamada, A. *Anal. Chim. Acta* **2000**, *405*, 87.
(36) Eramo, F. D.; Marioli, J. M.; Arevalo, A. H.; Sereno, L. E. *Talanta* **2003**, *61*, 341.
(37) Farrell, S. T.; Breslin, C. B. *Electrochim. Acta* **2004**, *49*, 4497.

JP109126Q